Reorganization Energies in the Transports of Holes and Electrons in Organic Amines in Organic Electroluminescence Studied by Density Functional Theory

Bo Chao Lin, Cheu Pyeng Cheng,* and Zhi Ping Michael Lao

Department of Chemistry, National Tsing Hua University, Sect. 2, Kuang-Fu Rd., Hsin Chu, 300, Taiwan

Received: April 16, 2003

To enable the design of efficient organic electroluminescence (OLED) devices with desirable charge carrier transport properties, the mobilities of hole and electron in a series of compounds were studied computationally based on the Marcus electron transfer theory. MO calculations were performed, using the DFT B3LYP/6-31G* method in the Gaussian 98 program suite, on the following compounds: biphenyl (Bp), 4,4′-biphenyldiamine (BA), triphenylamine (TPA), tri-*p*-tolylamine (TTA), 4-biphenylphenyl-*m*-tolylamine (BPTA), 4,4′-bis(phenyl-*m*-tolylamino)biphenyl (TPD), naphthalene (Np), 1-naphthyldiphenylamine (NDPA), 1-biphenylnaphthylphenylamine (BNPA), and 4,4′-bis(1-naphthylphenylamino)biphenyl (NPB). The geometries of these compounds in their neutral, cationic, and anionic states were optimized. The optimized geometries were then used to calculate the ionization potential, electron affinity, and reorganization energies. For compounds containing a biphenyl moiety (Bp, BA, BPTA, TPD, BNPA, and NPB), the inter-ring distance and torsional angle followed the trend neutral ≥ cationic ≥ anionic, except NPB in which these two parameters in anionic state were larger than the corresponding parameters in the cationic state because of a small contribution from the biphenyl moiety to its LUMO. Also, the ionization potentials follow the order Bp > BPTA ≈ BNPA > BA > NPB ≈ TPD. The electron affinities were calculated to range from −1.54 to −0.05 eV for all compounds except NPB which has a positive electron affinity 0.24 eV due to the dominant contribution of two naphthyl groups to LUMO. For most compounds, the reorganization energy λ_+ for the hole transport is larger than λ_- for the electron transport except NPB and BA_{py} (constrained nitrogen pyramidal geometry). These exceptions were rationalized by the special structures for their anionic states. According to the magnitudes of λ_+, compounds can be divided into two groups: $\lambda_+ \geq 0.28$ eV (BA_{pl} (constrained planar nitrogen geometry) ≈ Bp > TPD ≈ NPB) for compounds containing biphenyl group with or without two amino groups and $\lambda_+ \leq 0.2$ eV (TPA ≈ TTA < BPTA < BNPA ≈ NDPA) for compounds with single triarylamine group. According to the magnitudes of λ_-, compounds can be divided into three groups: $\lambda_- \geq 0.50$ eV (TPD > Bp > BPTA) for compounds with a dominating biphenyl group in their LUMO, $\lambda_- \leq 0.32$ eV (NDPA > BNPA > Np > NPB) for compounds with a dominating naphthyl group in their LUMO, and the other compounds (TPA and TTA). From these results, λ_+ is determined mainly by the moiety which contributes predominantly to its HOMO, whereas λ_- is determined mainly by the moiety which contributes predominantly to its LUMO. Therefore, by controlling the major contributors to the HOMO and LUMO, and by incorporating substituents to fine-tune the energy levels of these frontier orbitals (HOMO and LUMO), a systematic design of materials for OLED with desirable charge carrier transport properties should be feasible.

Introduction

Thin multilayer organic electroluminescence (OLED) device was recognized as one of the potential technologies for the next-generation flat-panel display devices since its discovery by Tang et al. in 1987.[1,2] Intensive research has been carried out to find the materials with high light emitting efficiencies, high thermal stability, and good amorphous film formation property.[3] The optoelectronic properties for OLED devices depend on appropriate HOMO and LUMO energy levels and suitable electron and hole mobilities. Although the guidelines for designing small molecules with the desirable photo[4] and thermal properties[5] are well-known, analogous guide on the mobilities of charge carriers in organic materials are limited because of the scarce of experimental data.[4,5] Nevertheless, the mobilities are important in optimizing the performance of OLED devices; high mobilities reduce the resistance of the device leading to high power

efficiency. In addition, the relative mobilities of electron and hole in the same material can also affect the power efficiency as described below.

One of the simplest OLED devices is a two layer device: ITO/HTL/ETL/Mg:Ag, in which HTL or/and ETL can act as light emitter. Holes are injected into HTL and migrate toward cathode upon applying voltage. Simultaneously, electrons are injected into ETL and migrate toward anode. Different combinations of the relative energies of HOMO and LUMO result in different major charge carriers crossing the interface. If the LUMO of HTL is much higher than that of ETL, then the barrier for the transport of electrons across the interface is high. If the HOMO of HTL is close to that of ETL, the barrier for the transport of holes across the interface is low. Under these situations, holes can migrate into ETL readily. Once the holes are transported across the interface, they can recombine with electrons to produce excitons leading to photon emission. The holes can also migrate toward the cathode leading to nonpro-
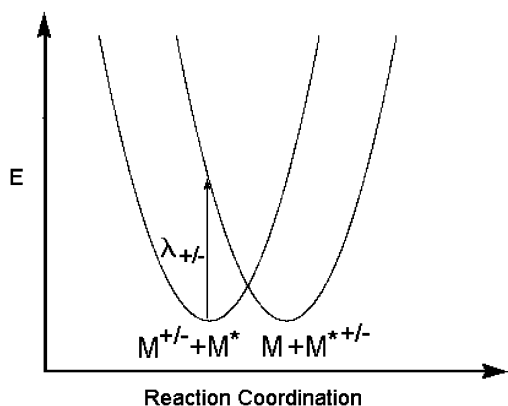
---

* To whom correspondence should be addressed.

Figure 1. Potential energy curves in the vertical transitions for the hole and electron transports.

Figure 2. Energies for a compound involved in the vertical transitions. The reorganization energy for hole transport λ_+ is given by $\lambda_1 + \lambda_2$; for electron transport, λ_- is given by $\lambda_3 + \lambda_4$.

ductive hole injection and consequently a waste of energy, thereby lowering the efficiency. The branching ratio of the desirable exciton formation and the undesirable migration toward the cathode depends on their respective rate constants. Although it remains unclear how to enhance the rate of exciton formation, a high branching ratio can be achieved if the mobility of the hole in ETL is low. Therefore, in this paper, we present a series of DFT calculations to further understand the factors influencing the mobilities of both electron and hole, which would be important for designing materials with high OLED efficiency.

The transports of charge carriers in amorphous organic solids can be rationalized in the formulizm of Gaussian disorders as first proposed by Bässler and co-worker.[8] In this formulizm, the mobilities depend on two key parameters: energy disorder and position disorder. It is difficult to relate these two disorder parameters to molecular properties to provide practical guidelines on the molecular level for designing suitable hole or electron transport material. From a different perspective, the transport of the electron or hole in the organic solid can also be viewed as an electron hopping process, which can be accounted for by the Marcus electron transfer theory.[9] The intermolecular transfer of hole and electron can be represented by eq 1

$$M^{+/-} + M^* \rightarrow M + M^{*+/-} \qquad (1)$$

In this eq, $M^{+/-}$ indicates the molecule in a cationic or anionic state. M^* is a neighboring molecule in a neutral state. The potential energy curve of this reaction is shown in Figure 1. The energy required for the vertical transition is $\lambda_{+/-}$. The rate of electron-transfer k_{et} is then given by eq 2

$$k_{et} = (4\pi^2/h)\,\Delta H_{ab}^{\,2}\,(4\pi\lambda_{+/-}T)^{-1/2}\exp(-\lambda_{+/-}/4kT) \quad (2)$$

ΔH_{ab} is the electronic coupling matrix element between donor and acceptor, k is the Boltzman constant, and h is the Planck constant. According to this equation, the thermal activation energies for the hole and electron-transfer processes are $\lambda_+/4$ and $\lambda_-/4$, respectively. Besides the terms involving $\lambda_{+/-}$, the ΔH_{ab} term also appears to be important for determining relative hole/electron transfer rates. However, experimentally determined ΔH_{ab} show a rather narrow range of values.[10] Based on the solution cationic intervalence spectra, the ΔH_{ab} were determined for a series of compounds with two hydrazine moieties connected by either aromatic or aliphatic bridges.[10] For the aromatic bridges in acetonitrile, ΔH_{ab} are 6.3, 3.1, and 3.8 kcal/ mol for 4,4′-phenyl, 4,4′-biphenyl, and 4,4′-durenyl, respectively. For a series of diverse aliphatic bridges, ΔH_{ab} are between 1.8 and 4.3 kcal/mol. These experimental results suggest a rather
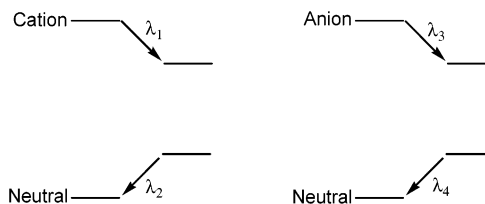
narrow range of values for ΔH_{ab}. Therefore, it is most likely that the ΔH_{ab} would also vary over a limited range for analogous bridges. Because the intermolecular charge-transfer processes considered in OLEDs involve direct contacts in amorphous solids, an even more limited range of ΔH_{ab} is expected. Therefore, based on this electron-transfer model, the mobilities of electrons and holes should be dominated by their respective reorganization energies λ_+ and λ_- in the exponential term in eq 2. In the vertical transitions, the reorganization energies are calculated according to the energy schemes shown in Figure 2. For hole transport, M^+ acquires an electron from M^* to become M which possesses the geometry of M^+. At the same time, M^* lost an electron to become M^{*+} which still assumes the geometry of M^*. Immediately after the vertical transition, M and M^{*+} are not in their lowest energy geometries. The sum of the relaxation energies toward their optimum geometries is then the reorganization energy; that is, λ_+ is given by $\lambda_1 + \lambda_2$. Similarly, in the electron transport process, M and M^{*-} are not in their lowest energy geometries immediately after the vertical transition. The sum of the energies λ_3 and λ_4 in the relaxation toward optimum geometries is the reorganization energy for the electron transport process; $\lambda_- = \lambda_3 + \lambda_4$. From λ_+ and λ_-, the activation energies for the hole and electron mobilities can be estimated.

There are only very few reports on the reorganization energies of organic materials. The reorganization energies of some amines $NMe_{3-n}Ph_n$ as hole transport materials have been calculated,[11] showing that the energy decreases with increasing n. For TPD, a well-known hole-transport material, λ_+, is dominated by the change of the torsional angle of the biphenyl group.[12] The charge transfers from biphenyl and 9,9′-dimethylfluorene anion radicals to several organic acceptors have been investigated by ab initio calculation showing that λ_-'s are greatly different depending on the species.[13] Although these pioneering MO studies have been important for understanding the transport of charge carriers in OLED materials on the molecular level, only one type of charge carrier was considered in these calculations. To gain a more comprehensive understanding, in this work, we report the reorganization energies of both holes and electrons for some arylamine containing compounds, including the widely used hole-transport materials such as TPD and NPB.

Experimental Section

All calculations were carried out at the DFT level using the B3LYP functional which employs the gradient corrected exchange functional with three parameters by Becke[14] and the correlation functional by Lee, Yang, and Parr.[15] The 6-31G* split valence plus polarization basis set is used.[16] The Gaussian 98 program suite[17] was used in all calculations. Molecular symmetries were used to facilitate our calculations where applicable.

Results and Discussion

To further understand hole and electron-transport properties in arylamine containing compounds, we performed DFT B3LYP/

Transports of Holes and Electrons in Organic Amines

J. Phys. Chem. A, Vol. 107, No. 26, 2003 **5243**

TABLE 1: Reorganization Energies of Biphenyl and TPD for Hole Transport λ_+/eV Calculated by Various Methods in the Gaussian 98 Program Suite

method				B3LYP			
basis set	AM1	STO-3G	3-21C	3-21G*	6-31G	6-31G*	6-31G**
biphenyl λ_-	0.446	0.618	0.642	0.641	0.542	0.559	0.561
λ_+	0.498	0.459	0.407	0.406	0.358	0.363	0.363
TPD λ_-		0.598	0.688	0.689	0.540	0.561	0.557
λ_+	0.710	0.232	0.275	0.274	0.272	0.281	0.283

6-31G* calculations on a series of compounds including biphenyl (Bp), 4,4′-biphenyldiamine (BA), triphenylamine (TPA), tri-*m*-tolylamine (TTA), 4-biphenylphenyl-*m*-tolylamine (BPTA), 4,4′-bis(phenyl-*m*-tolylamino)biphenyl (TPD), naphthalene (Np), 1-naphthyldiphenylamine (NDPA), 4-biphenyl-1-naphthylphenylamine (BNPA), and 4,4′-bis(*1*-naphthylphenylamino)biphenyl (NPB). Critical for understanding hole and electron-transfer properties are the corresponding reorganization energies (λ_+ and λ_-). The reorganization energies are the energies required in the process of the adjustments of geometries between the optimized geometries of compounds in their pertinent charged states (cationic and neutral for λ_+; anionic and neutral for λ_-). Therefore, the optimized geometries were calculated for the various charged states (cationic, anionic, and neutral). Also, the energies for the different charged states in the relevant geometries were obtained for calculating the reorganization energies for hole and electron transport. Besides the reorganization energies, other related energies including ionization potentials and electron affinities were also calculated.

The calculated values of λ_+ and λ_- are highly dependent on the method used as discussed below. For aniline, the λ_+ is 0.929 eV when calculated with HF/6-31G*.[11] However, its value is 0.529 eV when calculated with DFT B3LYP/3-21G*.[11] For biphenyl, λ_- is reported to be 1.123 eV when calculated with HF/6-31G*;[13] its value is 1.136 eV calculated with CAS/6-31G*.[13] To select an appropriate method to perfom this study, we carried out preliminary calculations on the reorganization energies of biphenyl and TPD for the transport of hole using AM1 and DFT B3LYP methods with various basis sets STO-3G, 3-21G, 3-21G*, 6-31G, 6-31G*, and 6-31G.** in the Gaussian 98 program suite. As expected, the reorganization energies λ_+ for hole transport in biphenyl and TPD depend on the choice of calculation method (Table 1). Calculations using AM1, B3LYP/STO-3G, B3LYP/3-21G, and B3LYP/3-21G* yield results quite different from those of B3LYP with the 6-31G type basis. Addition of polarizations yields similar results. Because calculations with the 6-31G** basis set are time-consuming and the yields that result are similar to that with 6-31G* basis set, therefore, we choose to use the 6-31G* basis set which is affordable in calculation time especially for molecules with a large number of atoms such as NPB.

Optimized Geometry. Because the results on the optimized geometries for TTA without symmetry constraint are similar to those for the corresponding triphenylamine, their geometries will not be shown below. The optimized geometries of naphthalene have been studied before.[13,18] The molecule remains planar, and only the C–H and C–C bond distances have some variations in different charge states. Therefore, its geometries will not be presented either.

A. Biphenyl (Bp). The inter-ring distances and the torsional angles in the optimized geometries of biphenyl in its neutral, cationic, and anionic states are collected in Table 2. The electron density isocontours of HOMO and LUMO are also appended to the table. The C_1–$C_1′$ distance 1.486 Å is in close agreement with that of the X-ray crystal data[19] and that of the gas-phase

TABLE 2: Inter-Ring Distances and Torsional Angles of Biphenyl in Its Neutral, Cationic, and Anionic States[a]
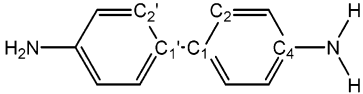

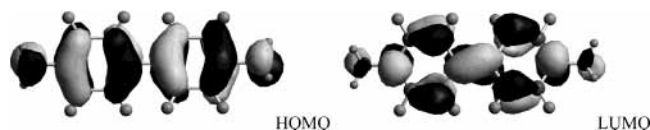|	C_1–$C_1′$/Å	torsional angle/°
neutral	1.486	38.4
cationic	1.443	19.5
anionic	1.439	5.8
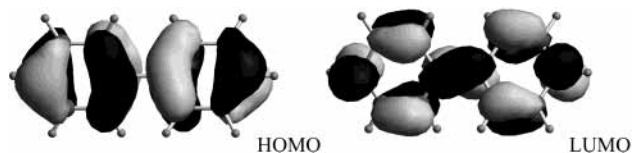
[a] Electron density isocontours (0.030 au) of HOMO and LUMO are included.

electron diffraction structure data.[20] This calculated inter-ring distance is also in agreement with those reported in recent theoretical studies.[11,13,21] Our calculated torsional angle 38.4° is quite different from that measured in the solid which is close to planar[18] and that in the gas phase 44.4°.[20] However, this torsional angle agrees well with other density functional calculations: 37.4°(BLYP/6-31G*);[21b] 38.3°(B3LYP/6-31G*);[21b] and 38.4°(B3LYP/6-31G**).[12] It is noteworthy that this angle is quite different from that calculated by the other ab initio methods: 44.3°(CASSCF);[30c] 42.6°(UHF/DZ);[21b] and 42.8°-(UHF/6-31G*).[13] In the cationic state, the inter-ring distance is 1.443 Å which is 0.04 Å shorter than that in its neutral state. This distance is in agreement with other theoretical studies: 1.44 Å (CASSCF)[22] and 1.44 Å (DFT B3LYP/6-31G**).[12] The torsional angle of 19.5° is in complete agreement with that reported by Bredas et al.[12] In the anionic state, the inter-ring distance is 1.439 Å which is slightly shorter than that in its cationic state. The torsional angle is 5.8° which is even smaller than that in its cationic state. The bond distances and torsional angles are similar to both experimental and theoretical results.[21b,23] The shortening of the inter-ring distances in cationic state relative to that in neutral state can easily be seen from the HOMO (−6.046 eV) of biphenyl in Table 2. The HOMO consists of the π orbitals from the two phenyl groups; each π orbital on the phenyl group is very similar to the HOMO of benzene with a nodal plane perpendicular to the C1–C1′ axis. There is an antibonding interaction between the π orbitals on the two phenyl rings. Hence, removing an electron from HOMO leads to a shortening of the inter-ring distance in the cationic state relative to the neutral state. The LUMO (−0.674 eV) of biphenyl consists of π orbitals of the two phenyl groups. Each of these π orbitals resemble the antibonding orbital of benzene in which two nodal planes are not perpendicular or parallel to the C1–C1′ axis. The shortening of the inter-ring distance in the anionic state is due to the bonding interactions between the π orbitals on the two phenyl groups.

B. 4,4′-Biphenyldiamine (BA). In geometrical optimization calculations, the results depend on the initial geometry around nitrogen atoms. With an initial pyramidal geometry of bond-angle 109.5°, the optimized geometries are pyramidal, planar and pyramidal for BA in neutral, cationic and anionic states, respectively. However, with an initial planar geometry, the final geometry is always planar regardless of charge. In the cationic state, the optimized geometry is always the same planar geometry no matter what are the initial geometries. The optimized pyramidal geometries are slightly more stable than

TABLE 3: Relevant Bond Distances, Bond Angles, and Torsional Angles of 4,4′-Diaminobiphenyl in Its Neutral, Cationic, and Anionic States[a]

		Amine with Pyramidal Geometry, BA$_{py}$.				
	C_1-C_1'/Å	$N-C_4$/Å	$C_2C_1C_1'C_2'$/°	$\angle HNH$/°	$\angle HNC_4$/°	sum[b]
neutral	1.482	1.400	36.4	111.0	114.5	340.0
cationic	1.445	1.384	17.6	117.0	121.5	360.0
anionic	1.439	1.444	0.0	105.8	109.4	324.6

HOMO LUMO

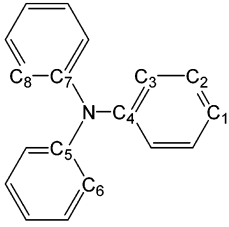|		Amine with Planar Geometry, BA$_{pl}$.				
	C_1-C_1'/Å	$N-C_4$/Å	$C_2C_1C_1'C_2'$/°	$\angle HNH$/°	$\angle HNC_4$/°	HNC_4C_3/°
neutral	1.482	1.380	36.1	117.8	121.1	0.0
cationic	1.445	1.348	17.7	117.0	121.5	0.5
anionic	1.439	1.421	6.7	116.6	121.7	65.9

HOMO LUMO
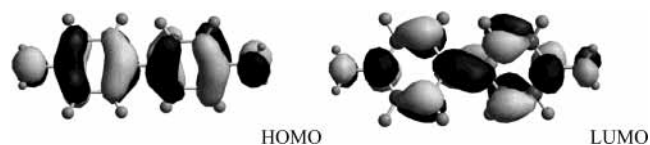
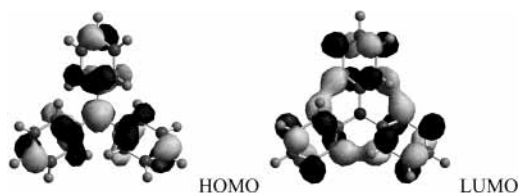[a] Electron density isocontours (0.030 au) of HOMO and LUMO are included. [b] Sum of angles around nitrogen.

the planar ones by an amount of 2.49 and 9.52 kcal for BA in the neutral and anionic state, respectively. The reason for including the planar geometries in this work is that it facilitates the comparison of the reorganization energies with the compounds containing triarylamine moieties which are always planar around nitrogen atoms.

The relevant bond distances, bond angles, and torsional angles of the optimized geometries together with the electron density isocontours of HOMO and LUMO of BA are collected in Table 3 for both the pyramidal (BA$_{py}$) and planar (BA$_{pl}$) amines. For BA$_{py}$, the inter-ring distances are 1.482, 1.445, and 1.439 Å in the neutral, cationic, and anionic states, respectively. These inter-ring distances are remarkably similar to the corresponding distances in biphenyl. The inter-ring torsional angles are 36.4°, 17.6°, and 0.0° in the neutral, cationic, and anionic states, respectively. These angles are also very close to the corresponding angles in biphenyl. The HOMO (−4.781 eV) and LUMO (0.005 eV) in Table 3 indicate that the major contributions come from the HOMO and LUMO of biphenyl. The orbitals of nitrogen atoms also make some contribution to both the HOMO and LUMO antibondingly. The fact that the $N-C_4$ distances are shortened in cationic state and lengthened in anionic state is consistent with the MO pictures. The sums of angles around nitrogen atoms are 340° for the neutral state and 324.6° for the anionic state.

For BA$_{pl}$, the inter-ring distance in any state is exactly the same as that in the corresponding ones in BA$_{py}$. The trends in $N-C_4$ distances and torsional angles are also remarkably similar to those in BA$_{py}$. Likewise, HOMO (−4.464 eV) and LUMO (0.279 eV) also resemble the corresponding ones in BA$_{py}$. However, the HNC_4C_3 torsional angle is strongly dependent on the charge on BA$_{pl}$, being 65.9° for the anionic state. Furthermore, there is a noticeable difference in reorganization energies between BA$_{py}$ and BA$_{pl}$ (vida infra).
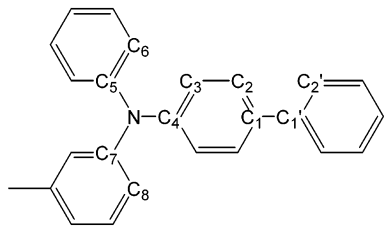
TABLE 4: Relevant Bond Distances, Bond Angles, and Torsional Angles of Triphenylamine in Its Neutral, Cationic and Anionic States[a]

|	$N-C_4$/Å	$\angle C_4NC_5$/°	$C_3C_4NC_5$/°
neutral	1.421	120.0	41.0
cationic	1.414	120.0	38.9
anionic[b]	1.420	120.0	40.8
anionic[c]	1.401, 1.424, 1.424	121.6, 121.6, 116.8	14.9, 57.8, 57.8

HOMO LUMO

[a] Electron density isocontours (0.030 au) of HOMO and LUMO are included. [b] C_3 symmetry imposed. [c] Without imposing C_3 symmetry.

C. Triphenylamine (TPA). The relevant bond distances, bond angles, and torsional angles of triphenylamine in the optimized geometries of its neutral, cationic, and anionic states together with the electron density isocontours of HOMO and LUMO are summarized in Table 4. The molecule, in any charged state, is always planar around the nitrogen atom as judged from the sum of angles around nitrogen. In the neutral state, the N−C distance 1.421 Å and torsional angle 41.0° are in excellent

Transports of Holes and Electrons in Organic Amines

J. Phys. Chem. A, Vol. 107, No. 26, 2003 **5245**

TABLE 5: Relevant Bond Distances, Bond Angles, and Torsional Angles of the Optimized Geometries of 4-Biphenylphenyl-*m*-tolylamine (BPTA) in Its Neutral, Cationic and Anionic States[a]

	N−C_4/Å	N−C_5/Å	N−C_7/Å	C_1−C_1'/Å	$C_3C_4NC_5$/deg	$C_6C_5NC_4$/deg	$C_8C_7NC_4$/deg	$C_2'C_1'C_1C_2$/deg
neutral	1.418	1.422	1.423	1.483	39.9	41.8	43.1	36.0
cationic	1.396	1.423	1.422	1.468	32.4	42.0	42.8	28.6
anionic	1.433	1.410	1.411	1.442	59.1	31.4	32.4	11.8

HOMO   LUMO
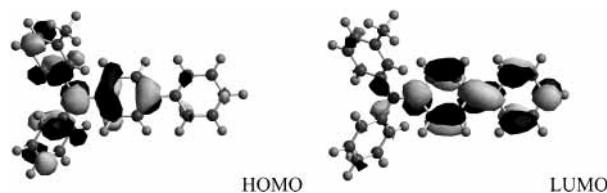
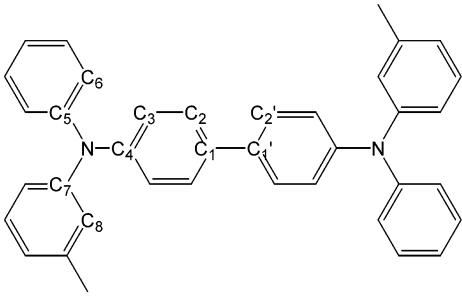[a] Electron density isocontours (0.030 au) of HOMO and LUMO are included.

agreement with the experimental crystal structure[24] and with the previous DFT[11,12] and ab initio HF[25] calculations. The HOMO (−4.948 eV) consists of the π orbitals of the three phenyl rings and the nitrogen p-orbital interacting antibondingly. The π orbital on each phenyl group resembles the HOMO of benzene with a modal plane perpendicular to the N−C axis. In the cationic form, the C−N distance 1.414 Å is shorter and the torsional angle 38.9° is smaller than the corresponding ones in the neutral state. This reduction can be seen from the HOMO. Removing an electron from HOMO will reduce the N−C antibonding interaction, leading to a shorter N−C distance. Simultaneously, the factor leading to the large torsional angle in neutral TPA is also reduced; consequently, the torsional angle is also reduced. We have also carried out calculation on TPA without symmetry constraint. Identical structural results are obtained in the cationic and neutral states.

In the anionic state, the total energy converges both in the presence and absence of the C_3 symmetry constraint. The total energy for the structure with C_3 symmetry is 0.91 kcal higher than the unrestrained structure. The geometrical parameters for both structures are included in Table 4. Under C_3 symmetry, the N−C_1 distance and phenyl ring torsional angle are very similar for the anionic and neutral states which can be attributed to the very week interaction between the π orbital of nitrogen and the π orbitals of the three phenyl groups in the LUMO (−0.297 eV). In TPA⁻ without C_3 symmetry, the three N−C bond distances are 1.042, 1.424, and 1.424 Å; the corresponding torsional angles are 14.9°, 57.8°, and 57.8°, respectively. This asymmetry can be explained by the TPA⁻ HOMO in which the π orbital of nitrogen strongly interacts with the π orbital of one phenyl ring bondingly and with the π orbitals of the other two phenyl rings antibondingly. Hence, one N−C bond is short, and the other two are long. Likewise one torsional angle is small, whereas the other two are large. This geometrical feature is in sharp contrast to the C_3 symmetrical prediction based on the isocontours of LUMO of neutral TPA.

We have also carried out calculations for tri-p-tolylamine. The geometries of C_3 symmetry constrained and nonconstrained are almost identical for neutral TTA as well as for cationic TTA⁺. The calculation for C3 symmetry constrained TTA⁻ does

not converge. Therefore, only results for unconstrained TTA⁻ will be presented in later section.(vide infra)

D. Biphenylphenyl-m-tolylamine (BPTA). In Table 5, the bond distances N−C_5 and N−C_7 are similar; likewise the torsional angles $C_6C_5NC_4$ and $C_8C_7NC_4$ are close to each other, in all states. It is then obvious that the presence of the methyl group in m-tolyl of BPTA makes negligible influence on its structure. The angles around nitrogen are 120.2°, 120.5°, and 119.3° for ∠C_4NC_5; 120.0°, 120.6, and 119.2° for ∠C_4NC_7; and 119.8°, 118.9°, and 121.6° for ∠C_5NC_7 for the neutral, cationic, and anionic states, respectively. Because the sums of the angles around the nitrogen atoms are 360° in all states, BPTA is planar around nitrogen. In the biphenyl moiety, the inter-ring distance C_1−C_1' and torsional angle $C_2'C_1'C_1C_2$ decrease on going from neutral to cationic then to anionic states. This trend is in agreement with those found in the optimized geometries in Bp and BA. The structural parameters of the tri-arylamine moiety are different from that of triphenylamine. In the neutral state, the N−C_4 distance is smaller than N−C_5 and N−C_7 distances. Also, the torsional angle $C_3C_4NC_7$ is smaller than those of C_6C_5-NC_4 and $C_8C_7NC_4$. In the cationic state, the N−C_4 distance and the torsional angle $C_4C_3NC_5$ are much smaller than those in the neutral state. In contrast, the distances N−C_5 and N−C_7 as well as the torsional angles $C_6C_5NC_4$ and $C_8C_7NC_4$ remain essentially the same in comparison to those for the neutral states. In the anionic state, the geometrical features are quite different from those calculated for TPA⁻ with or without C_3 symmetry constraint. The pattern is that N−C_4 becomes longer, and at the same time, N−C_5 and N−C_7 become shorter in comparison with those in its neutral state. The torsional angle $C_3C_4NC_5$ is much larger than those of $C_6C_5NC_4$ and $C_8C_7NC_4$. The HOMO (−4.883 eV) and LUMO (−0.738 eV) of BPTA consist of the contributions from the triarylamine and biphenyl moieties with a phenyl group common to both moieties. The changes of geometries in the cationic and anionic states are then those expected from those for the individual moieties on a somewhat reduced scale compared to TPA and BA. However, from the C_1−C_1' distances and $C_2'C_1'C_1C_2$ torsional angles, it can clearly be seen that the major geometrical differences between the anionic and neutral states are in the biphenyl moiety.

5246 *J. Phys. Chem. A, Vol. 107, No. 26, 2003*

Lin et al.

TABLE 6: Relevant Bond Distances, Bond Angles, and Torsional Angles in the Optimized Geometries of TPD in Its Neutral, Cationic, and Anionic State[a]
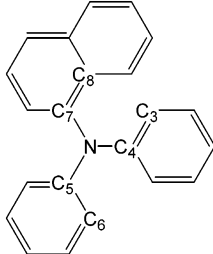

|	N−C$_4$/Å	N−C$_5$/Å	N−C$_7$/Å	C$_1$−C$_1'$/Å	C$_3$C$_4$NC$_5$/deg	C$_6$C$_5$NC$_4$/deg	C$_8$C$_7$NC$_4$/deg	C$_2'$C$_1'$C$_1$C$_2$/deg
neutral	1.419	1.422	1.423	1.480	41.4	40.9	42.7	34.8
cationic	1.387	1.431	1.432	1.455	25.8	48.8	49.3	22.4
anionic	1.436	1.411	1.411	1.441	61.4	31.2	31.7	9.1
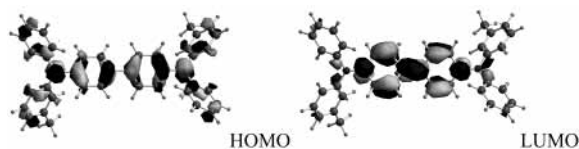
[a] Electron density isocontours (0.030 au) of HOMO and LUMO are included.

E. 4,4′-bis(phenyl-m-tolylamino)biphenyl (TPD). The angles around nitrogen are 120.0°, 121.1°, and 119.0° for ∠C$_4$NC$_5$; 120.1°, 121.1°, and 119.1° for ∠C$_4$NC$_7$; and 120.0°, 117.9°, and 121.9° for ∠C$_5$NC$_7$, for TPD in the neutral, cationic, and anionic states, respectively. Because the sums of the angles around nitrogen atoms are very close to 360° for TPD in all states, so their geometries must be planar around nitrogen. From the data of bond distances and bond angles in Table 6, it is clear that the methyl groups on tolyl groups have little effect on the structure of TPD in all states just as in the case of BPTA. In the biphenyl moiety, the inter-ring distance and the inter-ring torsional angle decrease on going from neutral, to cationic and then to anionic states just as in Bp, BA, and BPTA. These parameters are very similar to those of BPTA except the C$_1$−C$_1'$ distance and C$_2'$C$_1'$C$_1$C$_2$ torsional angle are noticeably smaller in the cationic state. In the triarylamine moiety, the structural parameters are very close to that of BPTA. In the anionic state, the pattern and magnitudes of the N−C distances and torsional angles or aryl groups are similar to those calculated for BPTA. Our geometrical parameters for TPD in the neutral and cationic states are in complete agreement with those of the other DFT/6-31G** calculations.[12] The HOMO (−4.684 eV) of TPD is a combination of the nitrogen π orbitals interacting antibondingly with the π orbitals of phenyl, tolyl, and biphenyl groups in which the biphenyl makes more significant contribution. The LUMO (−0.789 eV) is mostly concentrated on the biphenyl moiety with some contribution from the phenyl and tolyl groups.

F. 1-Naphthyldiphenylamine (NDPA). For NDPA, the angles around nitrogen are 121.3°, 119.9°, and 122.2° for ∠C$_4$NC$_5$; 119.5°, 121.0°, and 120.6° for ∠C$_4$NC$_7$; and 118.1°, 118.9°, and 117.1° for ∠C$_5$NC$_7$ for the neutral cationic and anionic states, respectively (Table 7). NDPA is planar around nitrogen atoms regardless of charge because the sums of angles around nitrogen atoms are very close to 360°. As expected, the two phenyl groups are not equivalent as indicated by the unequal N−C bond distances and torsional angles of these two phenyl groups with respect to the nitrogen plane because of the nonequivalent interactions with the naphthyl group. In the neutral state, the N−C$_7$ bond distance of the naphthyl group is
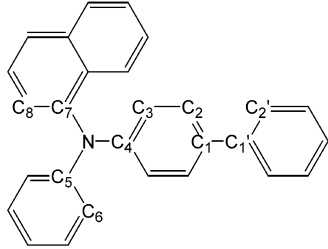
TABLE 7: Relevant Bond Distances and Torsional Angles of the Optimized Geometries of 1-Naphthyldiphenylamine (NDPA) in Its Neutral, Cationic, and Anionic States[a]

	N−C$_4$/ Å	N−C$_5$/ Å	N−C$_7$/ Å	C$_3$C$_4$NC$_5$/ deg	C$_6$C$_5$NC$_4$/ deg	C$_8$C$_7$NC$_4$/ deg
neutral	1.419	1.423	1.431	39.9	34.4	68.2
cationic	1.419	1.416	1.412	40.5	36.2	50.3
anionic	1.403	1.414	1.444	23.6	41.9	76.9
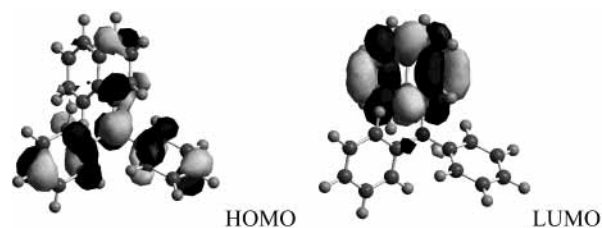
[a] Electron density isocontours (0.030 au) of HOMO and LUMO are included.

noticeably longer than the other two N−C distances. In the cationic state, the three N−C bond distances are about equal with N−C$_7$ slightly shorter. In the anionic state, the N−C$_7$ distance is also particularly long. The variation of the C−N$_7$ distance in the three states correlates with that of the torsional angle C$_8$C$_7$NC$_4$; the longer the distance the larger the torsional angle. The HOMO (−4.988 eV) of NDPA consists of nitrogen π orbital interacts in an antibonding fashion with the π orbitals on the three aryl groups. When an electron is removed from HOMO, N−C distances are shortened. In the LUMO (−1.103

Transports of Holes and Electrons in Organic Amines

J. Phys. Chem. A, Vol. 107, No. 26, 2003 **5247**

TABLE 8: Relevant Bond Distances and Torsional Angles of the Optimized Geometries of Biphenyl-*1*-naphthylphenylamine (BNPA) in Its Neutral, Cationic and Anionic States[a]

	N−C$_4$/Å	N−C$_5$/Å	N−C$_7$/Å	C$_1$−C$_1'$/Å	C$_3$C$_4$NC$_5$/deg	C$_6$C$_5$NC$_4$/deg	C$_8$C$_7$NC$_4$/deg	C$_2'$C$_1'$C$_1$C$_2$/deg
neutral	1.419	1.420	1.432	1.483	33.1	40.9	55.0	36.2
cationic	1.397	1.424	1.425	1.469	29.5	42.1	51.2	28.8
anionic	1.421	1.402	1.435	1.463	47.6	23.5	62.6	22.8
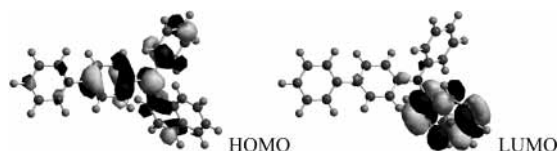
[a] Electron density isocontours (0.030 au) of HOMO and LUMO are included.

eV) of NDPA, the major contribution is the naphthyl π orbital together with small amount of π orbital of nitrogen.

G. Biphenyl-1-naphthylphenylamine (BNPA). In the optimized geometries of BNPA, the angles around nitrogen are 121.2°, 121.0°, and 121.8° for ∠C$_4$NC$_5$; 118.3°, 119.0°, and 116.8° for ∠C$_4$NC$_7$; and 119.5°, 119.8°, and 121.0° for ∠C$_5$NC$_7$ in the neutral cationic and anionic states, respectively. Because the sum of angles around nitrogen atoms are very close to 360°, it indicates that BNPA is planar regardless of its charge. From the optimized structural data in Table 8, the triarylamine moiety of BNPA in its neutral state and has N−C bond distances remarkably similar to those of the corresponding ones in NDPA in which one phenyl group is replaced by a biphenyl group. In the biphenyl moiety, the C$_1$−C$_1'$ distance and C$_2'$C$_1'$C$_1$C$_2$ torsional angle are also similar to those found in BDPA and TPD in the neutral state. In the cationic state, N−C$_4$ is particularly short in comparison to the other two N−C distances, but similar to that found for BPTA. The especially large torsional angle C$_8$C$_7$NC$_4$ (naphthyl) is similar to that found in BNPA. In the anionic state, the structural parameters in the amine moiety are similar to those of NDPA when the biphenyl group is treated as a phenyl group. However, in BNPA$^-$, the inter-ring distance and torsional angles are much larger than those in BPTA and TPD. These structural features are consistent with the HOMO (−4.946 eV) and LUMO (−1.148 eV) structures of BNPA. In the HOMO, the nitrogen π orbital interacts antibondingly with all aryl rings. The biphenyl makes a particularly large contribution. Therefore, when an electron is removed from HOMO, the N−C$_4$ becomes particularly short. The LUMO consists mainly of naphthyl LUMO. When an electron is added to the LUMO, the triarylamine moiety is not seriously affected; its structure is similar to those found in the neutral state. In both HOMO and LUMO, the π orbitals of the prime labeled phenyl groups in biphenyl make very small contributions. Consequently, C$_1$−C$_1'$ distances and torsional angles C$_2'$C$_1'$C$_1$C$_2$ do not vary a lot in different charged states as in Bp.

H. 4,4'-Bis(1-naphthylphenylamino)biphenyl (NPB). The geometries of NPB around nitrogen atoms are planar (sums of angles around nitrogen atoms, 359.5 ± 0.8°) no matter what is the charged state. From Table 9, the inter-ring distance is particularly short and the torsional angle is also particularly small

for NPB in its cationic state. In the triarylamine moiety, the N−C$_4$ (biphenyl) in NPB$^+$ is much shorter than those in NPB and NPB$^-$. Likewise, the torsional angle C$_3$C$_4$NC$_5$ is also noticeably smaller. In NPB$^-$, the N−C$_7$ (naphthyl) distance is particularly long in comparison with the other two N−C distances. These triarylamine structural variations of bond distances and torsional angles in Table 9 are similar to those in BNPA. The variations of the geometrical parameters can be seen from its HOMO (−4.732 eV) and LUMO (−1.145 eV). The HOMO consists of a major component of the biphenyl π orbitals with C$_1$ and C$_1'$ atomic π orbitals interact antibondingly with each other. The minor components of HOMO consist of the nitrogen π orbitals which strongly interact with the π orbital on C$_4$ antibondingly. In the LUMO, the major contribution comes from the π antibonding orbitals of the two naphthyl groups. Hence, in the anionic state, the geometrical parameters around nitrogen and biphenyl are similar to those in its neutral state.

Ionization Potential and Electron Affinity. The total energies (heat of formation) of the molecules in their optimized geometries in the neutral (assigned to a reference value 0.0 eV) and cationic states are shown in Figure 3. The energies of cations in neutral geometries and those of neutrals in the optimized cationic geometries are also included in the same figure. The data for tritolylamine (TTA) and naphthaline (Np), not discussed in the section of optimized geometries, are also included. The corresponding energies for anions are shown in Figure 4. The ionization potentials, Ip, differences in energies of cationic and neutral states in the optimized geometries for the neutral states, are given in Table 10. It is clear that our results of Ip on Bp, TPA, and TPD agree with those calculated by Bredas et al.[12] The Ip of TPA, calculated by the even more primitive 3-21G* basis set, also agrees well with our result.[11] However, the Ip of naphthalene calculated by the ab initio method using the 6-31+G* basis set[13] is about 0.4 eV higher than our result. Compared to experimental data, our calculated Ip's are low by one eV.

For compounds containing a biphenyl group, the order of Ip is Bp > BPTA > BNPA > BA$_{py}$ > BA$_{pl}$ > NPB ≈ TPD, indicating that Ip decreases as the number of amino groups in a compound increases. The presence of amino group(s) seems

TABLE 9: Relevant Bond Distances and Torsional Angles in the Optimized Geometries of 4,4′-Bis(1-naphthylphenylamino) Biphenyl (NPB) in Its Neutral, Cationic, and Anionic States[a]
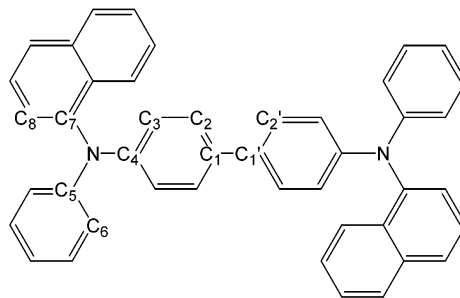
	N−C$_4$/Å	N−C$_5$/Å	N−C$_7$/Å	C$_1$−C$_1$′/Å	C$_3$C$_4$NC$_5$/deg	C$_6$C$_5$NC$_4$/deg	C$_8$C$_7$NC$_4$/deg	C$_2$′C$_1$′C$_1$/deg
neutral	1.421	1.420	1.431	1.482	33.0	40.8	54.9	35.3
cationic	1.388	1.430	1.438	1.457	22.8	45.7	59.9	19.8
anionic	1.423	1.407	1.434	1.473	44.3	28.0	60.8	27.7
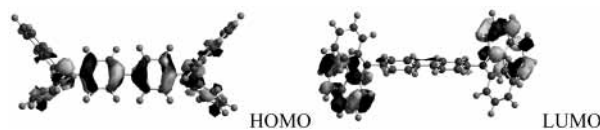
[a] Electron density isocontours (0.030 au) of HOMO and LUMO are included.

Figure 3. Energies in neutral and cationic states in the optimized geometries of the neutral and cationic states. Arrows indicate the reorganization energies λ_1 and λ_2 as those in Figure 2. TPA(a) and TTA(a) indicate TPA and TTA without C_3 symmetry constraint in DFT calculation.
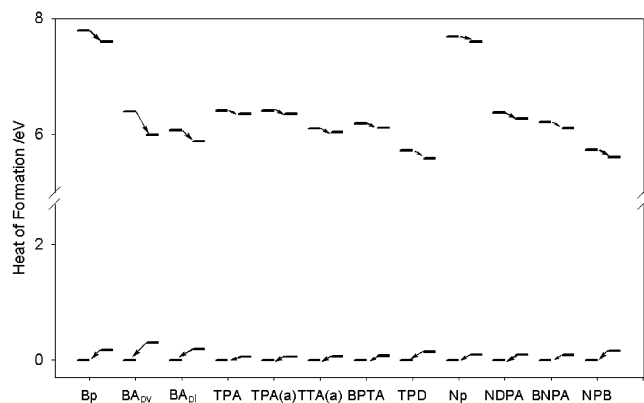

Figure 4. Energies in neutral and anionic states in the optimized geometries of the neutral and anionic states. Arrows indicate the reorganization energies λ_3 and λ_4 as those in Figure 2. TPA(a) and TTA(a) indicate TPA and TTA without C_3 symmetry constraint in DFT calculation.

to make HOMO higher. The higher Ip of TPA compared to that of TTA is obviously due to the electron donating effect of the methyl groups in TTA. The slightly larger Ip of NDPA than that of BNPA show that biphenyl group is more effective than phenyl group in lowering Ip.

The electron affinities, EA, the differences of the energies between neutral and their anionic states in the optimized geometry of neutrals, are also collected in Table 10. Our EA value for Np is higher by 0.5 eV than that calculated by the ab initio method with the 6-31G* basis set.[13] Interestingly, most of the calculated EA are negative except for NPB. The negative EA's originate from the incomplete cancellation of electronic self-interaction energy due to the use of inexact density functionals and a finite basis set.[33,34] Nevertheless, the relative magnitudes may still be useful for deducing general trends.[34] The positive EA for NPB is because it has two naphthyl groups to share the added electron. A general trend exists that the more aryl groups in the amine compounds, the higher the EA. In addition, the contribution of aryl groups to EA follow the order naphthyl > biphenyl > phenyl > tolyl. Application of the above two trends can account for the following orders of EA: (a) NPB
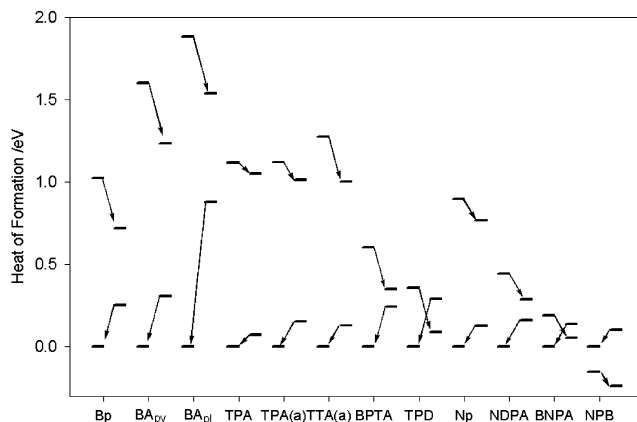
> TPD; (b) BNPA > NDPA; (c) BNPA > BPTP; (d) BPTA > TTA ≈ TPA.

Reorganization Energy. The reorganization energies λ_+ and λ_-, together with its components, λ_1, λ_2, λ_3, and λ_4, are collected in Table 11. Our calculated λ_+ for Bp, TPA, and TPD are in complete agreement with the data of Bredas et al.[12] However, our λ_- values are smaller than those calculated by ab initio CASSCF/6-31G* methods[13] by a factor of ca. 2 for Bp (0.26 vs 0.425 eV) and Np (0.56 vs 1.136 eV). Several general trends in Table 11 can be observed. The magnitudes of λ_1 and λ_2 are about equal for all compounds. Similarly, λ_3 is also about equal to λ_4 except for BA$_{pl}$. More interestingly, the magnitude of λ_+ is smaller than λ_- for all compounds in Table 11 except the data for BA$_{py}$ and NPB. Considering only the activation energies for electron hopping, our data indicate that Bp and Np and triarylamines, including the well-known hole transport material TPD, are better hole transporters than electron transporters. However, we are surprised by the result that NPB, also a well-known hole-transport material, is a better electron transporter rather than a hole transporter.

TABLE 10: Ionization Potentials Ip (Energy Difference between Cation and Neutral in the Optimized Geometry of Neutral) and Electron Affinities EA (Energy Difference between Neutral and Anion in the Optimized Geometry of Neutral) in eV

Cpd	Bp	BA_{py}	BA_{pl}	TPA^a	TPA^b	TTA^b	BPTA	TPD	Np	NDPA	BNPA	NPB
Ip	7.60	5.99	5.88	6.35	6.35	6.03	6.11	5.58	7.59	6.27	6.11	5.60
Ip^c	8.27[26]	7.1[28]	6.7[29]				6.69[31]	8.14[32]				
	8.34[27]		6.88[30]									
Ip^d	7.80[12]		6.4[11,12]				5.73[12]	7.99[13]				
	8.31[13]		6.42[12]									
EA	−0.72	−1.23	−1.54	−1.05	−1.01	−1.00	−0.34	−0.08	−0.77	−0.28	−0.05	0.23

^{a} With C_3 symmetry constraint. ^{b} No symmetry constraint. ^{c} Experimental Ip. ^{d} Other theoretical calculation.

TABLE 11: Reorganization Energies λ_+ and λ_-, Together with Its Components, λ_1, λ_2, λ_3, and λ_4 in eV Calculated by the DFT/B3LYP Method with the 6-31G* Basis Set

Cpd	Bp	BA_{pl}	BA_{py}	TPA^a	TPA^b	TTA^b	BPTA	TPD	Np	NDPA	BNPA	NPB
λ_+	0.36	0.38	0.71	0.12	0.12	0.13	0.15	0.28	0.18	0.20	0.19	0.29
λ_1	0.19	0.19	0.41	0.06	0.06	0.07	0.08	0.13	0.09	0.11	0.10	0.13
λ_2	0.17	0.19	0.30	0.06	0.06	0.06	0.08	0.15	0.09	0.09	0.09	0.16
λ_-	0.56	1.22	0.67	0.14	0.26	0.40	0.50	0.56	0.26	0.32	0.27	0.19
λ_3	0.31	0.34	0.37	0.07	0.11	0.27	0.25	0.27	0.13	0.16	0.14	0.09
λ_4	0.25	0.88	0.31	0.07	0.15	0.13	0.24	0.29	0.13	0.16	0.14	0.10
$k_{et+}/k_{et-}{}^c$	8.6	7200	0.66	1.3	5.7	24	54	21	2.6	4.0	2.68	0.31

^{a} Geometry constrained with C_3 symmetry. ^{b} Geometry without symmetry constraint. ^{c} Calculated for $T = 300$ K, neglecting differences in ΔH_{ab}.

In the reorganization process λ_1, the geometry changes from optimized neutral to optimized cation while the compound is in the cationic state. In the λ_2 process, the geometry change is the reverse of λ_1 while the compound is in the neutral state. Because these two processes involve the same geometrical change, it is reasonable to expect that λ_1 and λ_2 are comparable. Accordingly, the reorganization energies λ_3 and λ_4 should be similar. Apparently, BA_{pl} is an exception in which λ_4 is much larger than λ_3. This large difference can be explained upon careful examination of the geometric changes of the anionic and cationic states. In the λ_3 process (transition of the anionic species from the neutral geometry to the anionic geometry), the dihedral angles $C_2C_1C_1{}'C_2{}'$ and HNC_4C_3 change from 36.1° to 6.7° and from 0° to 69.5°, respectively, in the anioic state. In the λ_4 process, the directions in the geometrical changes are reversed with the molecule in the neutral state. From the LUMO of BA_{pl}, $N-C_4$ bonds are weakened facilitating the change of HNC_4C_3 dihedral angles in the anionic state. In contrast, the $C_1-C_1{}'$ bond is strengthened hampering the relaxation of the $C_2C_1C_1{}'C_2{}'$ dihedral angle. Therefore, the HNC_4C_3 dihedral angles adjustment for the λ_3 process occurs more readily than the λ_4 process. Furthermore, because there are a large changes in the HNC_4C_3 angle, both λ_3 and λ_4 processes should be dominated by this angle change. Consequently, λ_4 should be larger than λ_3 for BA_{pl}.

The values of λ_- for BA_{pl} and λ_+ and λ_- for BA_{py} are especially large compared to the corresponding values for the other compounds in Table 11. For BA_{pl}, λ_4 and λ_3 can be rationalized by geometric arguments as discussed earlier. The same arguments can explain the large value for λ_-. Furthermore, because the large HNC_4C_3 dihedral angle adjustment is not required in the λ_+ process for BA_{pl}, the reorganization energy is then comparable to that of Bp. When the geometrical adjustments of the pyramidal amino groups are not considered, BA_{py}, should have λ_+ and λ_- values comparable to Bp. Therefore, the large λ_+ and λ_- for BA_{py} can be attributed to the geometrical adjustments of both the pyramidal amino groups and biphenyl. Hence, direct comparison of the reorganization energies for BA_{py} and λ_- for BA_{pl} with other compounds in Table 11 may be misleading. The difference in λ_+ and λ_- for BA_{py} may be due to distinct geometrical adjustments for the corresponding transport of hole and electron. For hole transport, the reorganization (λ_1 and λ_2) involves adjustment of amino groups between a pyramidal structure and a planar structure together with changes in the biphenyl group. For electron transport, the reorganization energies (λ_3 and λ_4) involve adjustment of amino groups between a pyramidal structure and another pyramidal structure together with changes in the biphenyl group as well. On the basis of the extent of geometrical changes involved, it is likely that the geometrical adjustments in the λ_1 and λ_2 processes are more difficult than those of the λ_3 and λ_4 processes. Because of the complicating factors discussed above, the reorganization energies of BA_{py} and λ_- for BA_{pl} will not be further discussed.

According to the magnitude of λ_+, the compounds in Table 11 can be divided into two groups: one with $\lambda_+ \geq 0.28$ eV and the others with $\lambda_+ \leq 0.20$ eV. Compounds in each group share some common features. In the group with a large λ_+ value, the order of λ_+ is $BA_{pl} \approx Bp > TPD = NPB$. Compounds in this group have a biphenyl moiety with none or two amino groups attached to the biphenyl, and members of this group have a HOMO with major contribution from the biphenyl group. For TPD and NPB, the additional contributions from the diarylamino groups lower the λ_+'s. In the group with a small λ_+ value, the order is $TPA \approx TTA < BPTA < BNPA \approx NDPA$. Compounds in this group have a single triarylamine center; the HOMO of each member comprises mainly the π orbitals of nitrogen and the aryl groups. Additionally, the presence of the biphenyl group and the naphthyl group makes a more positive contribution to λ_+. However, Np is not included in the above grouping because no amine compounds in Table 11 have a HOMO with a major contribution from Np.

According to the magnitude of λ_-, we can divide the compounds in Table 11 into three groups. In the first group, λ_- is greater or equal to 0.50 eV, including $TPD \approx Bp > BPTA$. The LUMO of each compound in this group is mainly the antibonding orbital of biphenyl. In the second group, λ_- is equal to or less than 0.32 eV, including $NDPA > BNPA > Np > NPB$. Each compound in this group has a LUMO that is mainly the antibonding orbital of naphthalene. For NDPA and BNPA, the other constituting functional groups also contribute to the LUMO rising the λ_- over that of Np. The particularly small λ_- of NPB can be attributed to the presence of two naphthyl groups, both contributing equally to the LUMO of NPB. Each naphthyl

group shares the required geometrical reorganization after vertical transition. The third group includes TPA and TTA; their λ_- values cannot be categorized in the above two groups. The magnitude of λ_- of C_3 symmetry constrained TPA is significantly smaller than the unconstrained. This can be explained by detailed examination of the geometries of TPA$^-$ in the presence and absence of the symmetry constraint. The geometry of symmetry constrained TPA$^-$ resembles the optimized neutral structure; however, the geometry of unconstrained TPA$^-$ is significantly altered from the optimized neutral geometry. Hence, λ_- for symmetry constrained TPA is much smaller than that for unconstrained TPA. The magnitude of λ_- for TTA is larger than that of TPA because TTA is more electron rich, requiring more geometrical adjustment than TPA after acquiring an additional electron in vertical transition.

From the above analysis of the reorganization energies λ_+ and λ_-, it becomes clear that λ_+ is determined by the HOMO of the material, whereas λ_- is determined by its LUMO. Each moiety in a compound contributes to its HOMO and LUMO. The most significant moiety in the HOMO and LUMO determines roughly the magnitudes of λ_+ and λ_-. For example, the HOMOs in the group of compounds of Bp, BA$_{pl}$, TPD, and NPB consist mainly of the π orbital of the biphenyl moiety; therefore, the λ_+ values of these compounds are similar. In contrast, BPTA and BNPA, which also contain a biphenyl moiety, have a λ_+ value analogous to those for TPA and TTA. This is because the contribution of the biphenyl orbital to the HOMO of these monoamine compounds resembles that of a phenyl orbital. The presence of the diamino groups in BA$_{pl}$, TPD, and NPB pushes the biphenyl orbital higher to become the major contributor to their HOMOs. The same reasoning can also be applied to λ_-. For example, compounds containing a naphthyl group, such as NDPA, BNPA, and NPB, have a LUMO with a naphthyl orbital as the major component. Hence, these compounds have λ_- close to that of Np. Likewise, TPD, Bp, and BPTA have a LUMO dominated by the biphenyl π antibonding orbitals; they have approximately the same λ_-. One interesting comparison is the λ_+ and λ_- values of TPD and NPB. Both have a HOMO with a major contribution from the biphenyl orbital; they have the same value of λ_+. However, TPD has a LUMO with major contribution from the biphenyl orbital, whereas NPB has a major contribution from the naphthyl orbitals. Consequently, the λ_- value of NPB is 0.37 eV lower than that of TPD. This highlights the fact that the same constituent may play different roles in different compounds. For example, a biphenyl group may be the dominating factor in λ_+ for some compounds (BA$_{pl}$, TPD, and NPB), or be the dominating factor in λ_- for other compounds (TPD and BPTA), or have negligible effect in λ_- for another compounds (BNPA and NPB). Another example is the naphthyl group which has a major effect in λ_- of all compounds containing this functional group in Table 11, and has negligible effect in λ_+ for the same group of compounds. Therefore, it is misleading to predict the reorganization energy by the mere presence of a particular constituent in a compound. Instead, understanding the constituent's extent of contribution to HOMO and LUMO is necessary for predicting the reorganization energy.

We have established the relationships between λ_+ and HOMO as well as between λ_- and LUMO. The reorganization energies λ_+ and λ_-, should relate to geometrical adjustments between optimized cationic and neutral geometries for λ_+ and between optimized anionic and neutral geometries for λ_-. However, the cationic geometry is intimately related to HOMO and the anionic geometry to LUMO. A simplistic view would directly relate

the reorganization energies to the HOMO and LUMO. Amazingly, this simplistic view is consistent with our findings. Because the basic principles for modifying these HOMO and LUMO energetics are well-known, the same guidelines may be applied to altering the reorganization energies for designing OLEDs with predictable charge carrier transport properties. One should be careful that there may be situation in which the geometry of anion or cation may be different from that predicted by LUMO and HOMO as in the geometries of TPA$^-$ and TTA$^-$ unconstrained by symmetry.

To compare the magnitudes of hole and electron mobilities, we calculate the relative hopping rates of holes versus electrons, k_{et+}/k_{et-}, according to $(\lambda_-/\lambda_+)^{1/2}\exp[(\lambda_- - \lambda_+)/4kT]$ assuming T to be 300 K and neglecting the difference in ΔH_{ab}, (Table 11). The ratio is predicted to be 23 for TPD and 0.31 for NPB. Although some experimental data indicated that ΔH_{ab} varies over a rather limited range for intramolecular charge-transfer processes,[10] this does not guarantee complete cancellation in the comparison of relative charge-transfer rates. Furthermore, the range of ΔH_{ab} for intermolecular charge-transfer processes for amines in solids remains unknown and is therefore currently under theoretical investigation in our lab.

The hole mobilities of TPD[4a,c,g] and NPB[4c,e,5d] have been reported to be on the order of 10^{-4} cm^2 V^{-1} s^{-1}. However, direct comparison of their reported mobilities is not appropriate because the values depend on the electric field and film preparation details, such as, rate of vacuum deposition.[4d] Unfortunately, there has no report on the electron mobility for NPB except for a failed attempt because of a weak signal.[4e] Therefore, future experimental studies are necessary to confirm our predictions based on the calculations without considering the difference in ΔH_{ab}. Also, the relative contribution of ΔH_{ab} is currently under theoretical investigation in our lab to provide more accurate predictions.

Conclusion

Our DFT B3LYP/6-31G* calculations on a series of compounds containing triarylamine moieties together with simple molecules Bp and Np, have revealed that the reorganization energies, λ_+ and λ_-, are determined by some simple rules. The reorganization energy for hole transport (λ_+) is controlled by HOMO. Therefore, the major contributor to HOMO in the constituent moieties of a given compound determines the magnitude of λ_+ with some modification due to the presence of the other moieties. Similarly, the reorganization energy λ_- for the electron transport is controlled by LUMO. Based on these results, we can formulate a procedure in predicting the magnitude of reorganization energies. A list of λ_+ and λ_- for the components in a materials is required for the prediction. The reorganization energies of a material can be inferred from those of its components. If there is a major contributor to the HOMO or LUMO, then λ_+ or λ_- is close to that particular contributor. Systematic alterations on the molecular level can be employed for achieving a particular reorganization energy. For example, substituent(s) can be used to raise or lower the energy of a particular constituent. In addition, one can construct a material in such a fashion that λ_+ is controlled by one component while λ_- is controlled by another component. By this differential control on the reorganization energies, one can design compounds with desired transport properties. In particular, ideal hole transporting compounds with large λ_- and small λ_+ or electron transporting compounds with large λ_+ and small λ_- can be realized for future development of OLEDs and other optoelectric materials.

Transports of Holes and Electrons in Organic Amines

J. Phys. Chem. A, Vol. 107, No. 26, 2003 **5251**

References and Notes

(1) Tang, C. W.; Van Slyke, S. A. *Appl. Phs. Lett.* **1987**, *51*, 913.

(2) (a) Van Slyke, S. A.; Tang, C. W. U.S. Patent No. 4,539,507, 1985. (b) Tang, C. W.; Van Slyke, S. A.; Chen, C. H. *J. Appl. Phys.* **1989**, *65*, 3610.

(3) (a) Shirota, Y.; Okumoto, K.; Inada, H. *Synth. Met.* **2000**, *111*, 387. (b) Wu, I.-Y.; Lin, J. T.; Tao, Y.-T.; Balasubramaniam, E.; Su, Y. Z.; Ko, C.-W. *Chem. Mater.* **2001**, *13*, 2626. (c) Salbeck, J.; Yu, N.; Bauer, J.; Weissotel, F.; Bestgen, H. *Synth. Met.* **1997**, *91*, 209. (d) Maiti, B. C.; Wang, S. Z.; Cheng, C. P.; Huang, D. J.; Chao, C.-I. *J. Chin. Chem. Soc.* **2001**, *48*, 1059.

(4) (a) Wehry, E. L. *Effects of Molecular Structure on Fluorescence and Phosphorescence* in *Practical Fluorescence*, 2nd ed.; Guilbault, G. C., Ed.; Marcel Dekker: New York, 1990. (b) Valeur, B. *Molecular Fluorescence Principles and Applications*; Wiley-VCH: Weinheim, Germany, 2002.

(5) Naito, K.; Miura, A. *J. Phys. Chem.* **1993**, *97*, 6240.

(6) (a) Fong, H. H.; Lun, K. C.; So, S. K. *Chem. Phys. Lett.* **2002**, *353*, 407. (b) Era, M.; Kakiyama, N.; Noto, M.; Lee, S. H.; Tsutsui, T. *Mol. Cryst. Liq. Cryst.* **2001**, *371*, 191. (c) Naka, S.; Okada, H.; Onnagawa, H.; Yamaguchi, Y.; Tsutsui, T. *Synth. Met.* **2000**, *111−112*, 331. (d) Chen, B. J.; Lai, W. Y.; Gao, Z. Q.; Lee, C. S.; Lee, S. T.; Gambling, W. A. *Appl. Phys. Lett.* **1999**, *75*, 4010. (e) Deng, Z.; Lee, S. T.; Webb, D. P.; Chan, Y. C.; Gambling, W. A. *Synth. Met.* **1999**, *107*, 107. (f) Kepler, R. G.; Beeson, P. M.; Jacobs, S. J.; Anderson, R. A.; Sinclair, M. B.; Valencia, V. S.; Cahill, P. A. *Appl. Phys. Lett.* **1995**, *66*, 3618. (g) Mori, M.; Sugimura, E.; Mizutani, T. *J. Phys. D* **1993**, *26*, 452.

(7) (a) Kawabe, Y.; Abe, J. *Appl. Phys. Lett.* **2002**, *81*, 493. (b) Xie, Z.-Y.; Wong, T.-C.; Hung, L.-S.; Lee, S.-T. *Appl. Phys. Lett.* **2002**, *80*, 1477. (c) Wong, T. C.; Kovac, J.; Lee, C. S.; Hung, L. S.; Lee, S. T. *Chem. Phys. Lett.* **2001**, *334*, 61. (d) Kovac, J.; Wong, T. C.; Fung, M. K.; Liu, M. W.; Kremnican, V.; Bello, I.; Lee, S. T. *Mater. Sci. Eng.* **2001**, *B85*, 172. (e) Barth, S.; Muller, P.; Riel, H.; Seidler, P. F.; Riess, W.; Vestweber, H.; Bassler, H. *J. Appl. Phys.* **2001**, *89*, 3711. (f) Lee, C. H.; Kang, G. W.; Jeon, J. W.; Song, W. J.; Seoul, C. *Thin Solid Films* **2000**, *363*, 306. (g) Hosokawa, C.; Tokailin, H.; Higashi, H.; Kusumoto, T. *Appl. Phys. Lett.* **1993**, *60*, 1220.

(8) (a) Bässler, H. *Phys. Stat. Sol. B* **1993**, *175*, 15. (b) Stolka, M.; Yanus, J. F.; Pai, D. M. *J. Phys. Chem.* **1984**, *88*, 4707. (c) Lebedev, E.; Dittrich, T.; Petrova-Koch, V.; Karg, S.; Brutting, W. *Appl. Phys. Lett.* **1997**, *71*, 2686. (d) Fong, H. H.; Lun, K. C.; So, S. K.; *Chem. Phys. Lett.* **2002**, *353*, 407. (e) Borsenberger, P. M.; Weiss, D. S. *Organic Photoreceptor for Xeroxgraphy*; Marcel Dekker: New York, 1998; Chapter 7.

(9) (a) Marcus, R. A. *J. Chem. Phys.* **1956**, 24, 966. (b) Marcus, R. A. *J. Chem. Phys.* **1965**, *43*, 679. (c) Newton, M. D.; Sutin, N. *Annual Rev. Phys. Chem.* **1984**, *35*, 437. (d) Marcus, R. A.; Sutin, N. *Biochim. Biophys. Acta* **1985**, *811*, 265. (e) Barbara, P. F.; Meyer, T. J.; Ratner, M. A. *J. Phys. Chem.* **1996**, *100*, 13148.

(10) (a) Nelsen, S. F.; Trieber, D. A., II.; Ismagilov, R. F.; Teki, Y. *J. Am. Chem. Soc.* **2001**, *123*, 5684−5694. (b) Nelsen, S. F.; Blomgren, F. *J. Org. Chem.* **2001**, *66*, 6551−6559.

(11) Sakanoue, K.; Motoda, M.; Sugimoto, M.; Sakaki, S. *J. Phys. Chem. A* **1999**, *103*, 5551.

(12) Malagoli, M.; Bredas, J. L. *Chem. Phys. Lett.* **2000**, *327*, 13.

(13) Li, X.-Y.; Tong, J.; He, F.-C. *Chem. Phys.* **2000**, *260*, 283.

(14) (a) Becke, A. D. *Phys. Rev. A* **1988**, *38*, 3098. (b) Becke, A. D. *J. Chem. Phys.* **1993**, *98*, 5648.

(15) Lee, C.; Yang, W.; Parr, R. G. *Phys. Rev. B* **1988**, *37*, 785.

(16) (a) Ditchfield, R.; Hehre, W. J.; Pople, J. A. *J. Chem. Phys.* **1971**, *54*, 724. (b) Hehre, W. J.; Dichfield, R.; Pople, J. A. *J. Chem. Phys.* **1972**, *56*, 2257. (c) Hariharan, P. C.; Pople, J. A. *Mol. Phys.* **1974**, *27*, 209. (d) Gordon, M. S. *Chem. Phys. Lett.* **1980**, *76*, 163. (e) Hariharan, P. C.; Pople, J. A. *Theor. Chim. Acta* **1973**, *28*, 213.

(17) Frisch, M. J.; Trucks, G. W.; Schlegel, H. B.; Scuseria, G. E.; Robb, M. A.; Cheeseman, J. R.; Zakrzewski, V. G.; Montgomery, J. A., Jr.; Stratmann, R. E.; Burant, J. C.; Dapprich, S.; Millam, J. M.; Daniels, A. D.; Kudin, K. N.; Strain, M. C.; Farkas, O.; Tomasi, J.; Barone, V.; Cossi, M.; Cammi, R.; Mennucci, B.; Pomelli, C.; Adamo, C.; Clifford, S.; Ochterski, J.; Petersson, G. A.; Ayala, P. Y.; Cui, Q.; Morokuma, K.; Malick, D. K.; Rabuck, A. D.; Raghavachari, K.; Foresman, J. B.; Cioslowski, J.; Ortiz, J. V.; Stefanov, B. B.; Liu, G.; Liashenko, A.; Piskorz, P.; Komaromi, I.; Gomperts, R.; Martin, R. L.; Fox, D. J.; Keith, T.; Al-Laham, M. A.; Peng, C. Y.; Nanayakkara, A.; Gonzalez, C.; Challacombe, M.; Gill, P. M. W.; Johnson, B. G.; Chen, W.; Wong, M. W.; Andres, J. L.; Head-Gordon, M.; Replogle, E. S.; Pople, J. A. *Gaussian 98*, revision 1.1; Gaussian, Inc.: Pittsburgh, PA, 1998.

(18) Monella, M. *J. Mol. Struct. (THEOCHEM)* **1996**, *362*, 7.

(19) Cailleau, H.; Baudour, J. L.; Zeyen, C. M. E. *Acta Crystallogr. B* **1979**, *35*, 426.

(20) Almenningen, A.; Bastiansen, O.; Fernholt, L.; Cyvin, B. N.; Cyvin, S. J. *J. Mol. Struct.* **1985**, *128*, 59.

(21) (a) Tsuzuki, S.; Tanabe, K. *J. Phys. Chem.* **1991**, *95*, 139. (b) Furuya, K.; Torii, H.; Furukawa, Y.; Tasumi, M. *J. Mol. Struct. (THEOCHEM)* **1998**, *424*, 225. (c) Rubio, M.; Merchan, M.; Orti, E. *THEOCHEM* **1995**, *91*, 17. (d) Li, X.-Y.; Xia, S.-Q.; He, F.-C. *Sci. Chin.* **1999**, *42*, 441.

(22) Rubio, M.; Merchan, M.; Orti, E.; Roos, B. O. *J. Phys. Chem.* **1995**, *99*, 4980.

(23) (a) Takei, Y.; Yamaguchi, T.; Osamura, Y.; Fuke, K.; Kaya, K. *J. Phys. Chem.* **1988**, *92*, 577. (b) Buntinx, G.; Poizat, O. *J. Chem. Phys.* **1989**, *91*, 2153.

(24) Sobolev, A. N.; Bel'skii, V. K.; Romm, I. P.; Chernikov, N. Y.; Guryanova, E. N. *Acta Crystallogr.* **1985**, *C41*, 967.

(25) Pacansky, J.; Waltman, R.; Seki, H. *Bull. Chem. Soc. Jpn.* **1997**, *70*, 55.

(26) West, R. C., Astle, M. J., Ed.; *CRC Handbook of Chemistry and Physics*, 63rd ed.; CRC Press: Boca Raton, FL, 1982; p E-63.

(27) Ruscic, R.; Kovac, B.; Klasinc, L.; Gusten, H. *Z. Naturforsch*, **1978**, *A33*, 1006.

(28) Kalnin'sh, K. K.; Safant'evskii, A. A.; Roshchina, E. K.; Petrov, L. N. *Bull. Acad. Sci. USSR Div. Chem. Sci.* **1987**, *36*, 2276.

(29) (a) Crable, G. F.; Kearns, G. L. *J. Phys. Chem.* **1962**, *66*, 436. (b) Farrell, P. G.; Newton, J. *J. Phys. Chem.* **1965**, *69*, 3506.

(30) Meijer, G.; Berden, G.; Meerts, W. L.; Hunziker, H.; de Vries, M. S.; Wendt, H. R. *Chem. Phys.* **1992**, *163*, 209.

(31) Anderson, J. D.; McDonald, E. M.; Lee, P. A.; Anderson, M. L.; Ritchie, E. L.; Hall, H. K.; Hopkins, T.; Mash, E. A.; Wang, J.; Padias, A.; Thayumanavan, S.; Barlow, S.; Marder, S. R.; Jabbour, G. E.; Shaheen, S.; Kippelen, B.; Peyghambarian, R.; Wightman, R. M.; Armstrong, N. R. *J. Am. Chem. Soc.* **1998**, *120*, 9646.

(32) (a) Crowell, R. A.; Trifunac, A. D. *J. Phys. Chem. A* **1998**, *102*, 4976. (b) Cockett, M. C. R.; Ozeki, H.; Okuyama, K.; Kimura, K. *J. Chem. Phys.* **1993**, *98*, 7763.

(33) Rienstra-Kiracofe, J. C.; Tschumper, G. S.; Schaefer, H. F., III.; Nandi, S.; Ellison, G. B. *Chem. Rev.* **2002**, *102*, 231−282 and references therein.

(34) It should be noted EAs of some compounds are actually negative; see, for example: Li, X.; Cai, Z.; Sevilla, M. D. *J. Phys. Chem. A* **2002**, *106*, 1596−1603.